www.czasopisma.pan.pl PAN www.journals.pan.pl
Chemical and Process Engineering 2018, 39 (3), 295–308
DOI: 10.24425/122951

SHORT COMMUNICATION

CERAMIC MEMBRANE FOULING IN ULTRAFILTRATION PROCESS OF CHICKEN EGG WHITE AQUEOUS SOLUTION

Martyna Borysiak, Elżbieta Gabruś*

West Pomeranian University of Technology, Szczecin, Faculty of Chemical Technology and Engineering, Institute of Chemical Engineering and Environmental Protection Processes, al. Piastów 42, 71-065 Szczecin, Poland

This paper presents an experimental study on chicken egg white solution ultrafiltration, where membrane fouling has been the main point of concern. Separation process has been performed with a 150 kDa tubular ceramic TiO_2/Al_2O_3 membrane. The operating parameters have been set as follows: transmembrane pressure 105–310 kPa, cross-flow velocity 2.73–4.55 m/s, pH 5 and constant temperature of 293 K. Resistance-in-series model has been used to calculate total resistance and its components. The experimental data have been described with four pore blocking models (complete blocking, intermediate blocking, standard blocking and cake filtration). The results obtained show that the dominant fouling mechanism is represented by cake filtration model.

Keywords: ultrafiltration, ceramic membrane, chicken egg white, fouling, membrane transport resistance

1. INTRODUCTION

Separation of macromolecular solutions (e.g. polysaccharides, proteins in water) is broadly realized through low pressure filtration processes. Among them we can distinguish microfiltration (MF) and ultrafiltration (UF). The driving force of these processes is transmembrane pressure. Micro- and ultrafiltration membranes are made from porous materials and separation is realized through sieve mechanism (Bodzek et al., 1997; Fane et al., 2011; Pabby et al., 2008). Microfiltration membranes are symmetric and their pore size is defined by diameter measured in micrometers, while ultrafiltration pores are asymmetric and their size is expressed with molecular weight in Daltons (Bodzek et al., 1997).

One of the main problems that occur in membrane processes is membrane fouling, which causes a decrease of permeate flux during filtration. There are several possible mechanisms that may be considered responsible for this phenomenon. Generally, when a solution containing macromolecules enters a membrane unit, the solvent and molecules smaller than the pores pass through, while the molecules equal and bigger than the pores size are stopped. Membrane pores can be blocked in several possible ways according to the appropriate models. The molecules can either block the pore entrances, get adsorbed on the pores surface, limit the pores volume or form a cake layer (Hermia, 1985; Vincent Vela et al., 2009). These mechanisms have been discussed in detail later in the paper. Fouling is an undesirable phenomenon that is very difficult to avoid, so researching the mechanisms and the ability to calculate and predict the re-

* Corresponding author, e-mail: Elzbieta.Gabrus@zut.edu.pl
Reprinted with permission in an extended form from the EYEC Monograph accompanying 7th European Young Engineers Conference. *http://journals.pan.pl/dlibra/journal/98834*

sistances of mass transport is crucial for membrane system designs and applications (Balyan and Sarkar, 2018; Corbatón-Báguena et al., 2015; Corbatón-Báguena et al., 2018; Kumar et al., 2016).

One of the main areas where ceramic membranes are used is food processing industry (Samaei et al., 2018). Separation of proteins, polysaccharides etc. from wine (Li et al., 2010; Rayess et al., 2011; Youravong et al., 2010), wastewaters (Agana et al., 2013; Yin et al., 2013), fruit and vegetable juices (Almandoz et al., 2010; de Barros et al., 2003), as well as bovine serum albumin (Huisman et al., 2000; Muca et al., 2017; Prádanos et al., 1996) has been studied by many authors. Fractionation and purification of chicken egg white components (e.g. ovalbumin, lysozyme) from single and multiple protein solutions (protein in water, fresh chicken egg white, BSA/lysozyme binary solution etc.) has been successfully attempted with membranes made of polymeric materials (Ehsani et al., 1997; Ghosh and Cui, 1998; Jana et al., 2011; Lu et al., 2005; Lu et al., 2006; Muca et al., 2017; Tung et al., 2007; Wan et al., 2006), regenerated cellulose (Lu et al., 2005; Wan et al., 2006) and inorganic materials (Matsumoto et al., 1996).

The aims of this work are: estimating the resistances that occur during chicken egg white ultrafiltration, analysis of fouling mechanisms; identifying the dominant fouling mechanism in ultrafiltration of chicken egg white solution.

2. MATERIALS AND METHODS

2.1. Membrane system

The membrane unit consisted of a feed tank, a pump, a membrane module, a rotameter, a tubular heat exchanger for stabilizing the temperature, a permeate tank, scales and a computer. Retentate stream was being recirculated back to the feed tank, while permeate stream was being collected in the permeate tank placed on scales linked to a computer. The scales' readings were saved in DasyLAB software with a 15 second interval. Experimental setup with membrane unit is shown in Fig. 1.

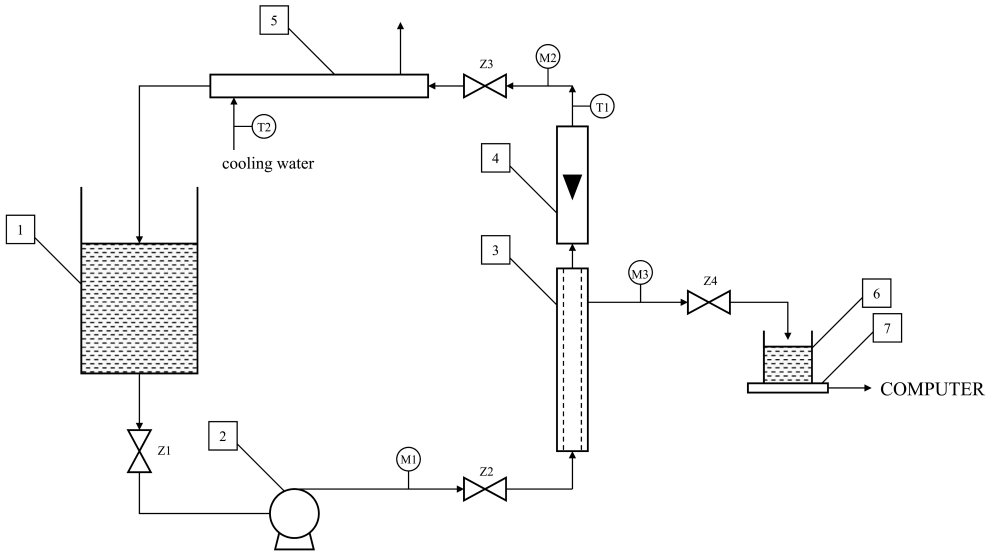

Fig. 1. Experimental setup with membrane unit; 1 – feed solution tank, 2 – pump, 3 – membrane unit, 4 – rotameter, 5 – tubular heat exchanger, 6 – permeate tank, 7 – scales linked to a computer

The experiments were conducted with a 3-channel 150 kDa tubular ceramic TiO_2/Al_2O_3 membrane (Tami Industries, France), placed in a stainless steel module. Complete characteristic parameters of the membrane are listed in Table 1.

Table 1. Ceramic membrane parameters

Type	Clover, 3-channel
Molecular weight cut-off	150 kDa
Separation area	0.009375 m^2
Length	0.25 m
Outer diameter	0.01 m
Single channel hydraulic diameter	0.0036 m
Max. temperature	< 150 °C
pH range	0–14
Destructive pressure	> 9 MPa

Severe fouling formed during ultrafiltration of protein solutions ought to be removed chemically. Ceramic membranes, which are often used for protein separation, are more resistant to high temperatures and aggressive chemical environment than those made of polymeric materials, which is why this type has been chosen for research, despite the higher cost of production (Pabby et al., 2008). Its high temperatures resistance also allows for steam sterilization, which combined with chemical cleaning regime, can be regarded sufficient for biohazardous particle removal.

2.2. Protein solution

Powdered chicken egg white purchased from Egg Factory "Ovopol" (Poland) has been used as a protein in experiments. Chicken egg white is not a single protein, but consists of a few proteins – the main one is ovalbumin (54–57% (Wan et al., 2006)) and its physical properties were taken into account. Concentration of the solute in the feed stream has been set to 0.2 g/L. Physical properties of this protein and its aqueous solution with the given concentration are given in Table 2. As pH adjustment factors, 0.1 M NaOH and 0.1 M HCl have been used. Values of pH have been measured with MERA-ELMET N5122 universal pH-meter.

Table 2. Chicken egg white aqueous solution properties

molecular weight	45 kDa (Wan et al., 2006)
isoelectric point	4.5 (Wan et al., 2006)
concentration	0.2 g/L
diffusion coefficient	1.18×10^{-10} m^2/s (Wan et al., 2006)
density	1001 kg/m^3 (Gabruś, 2016)
dynamic viscosity	1.12×10^{-3} Pa·s (Gabruś, 2016)
pH	5

Concentration of solute in feed (C_F) and permeate (C_P) stream has been determined via absorbance (wavelength equal to 280 nm) measured with a SHIMADZU UVMINI-1240 spectrophotometer.

Operating parameters of the test runs are listed in Table 3. All of the measurements have been carried out at 293 K. Each measurement lasted 80–100 minutes to acquire the pseudo steady-state flux. Each time

directly after a single measurement, water permeation measurement was carried out. Then a chemical cleaning process has been conducted to remove the protein particles remaining on the membrane surface.

Table 3. Chicken egg white ultrafiltration mass transport resistances, hydraulic permeability and retention coefficient values

u [m/s]	TMP [kPa]	$R_T \cdot 10^{-12}$ [1/m]	$R_M \cdot 10^{-12}$ [1/m]	$R_F \cdot 10^{-12}$ [1/m]	$R_{RES} \cdot 10^{-11}$ [1/m]	R_F/R_T	$L_M \cdot 10^{10}$ [m^3/(m^{2}sPa)]	$L_P \cdot 10^{10}$ [m^3/(m^{2}sPa)]	R_{coef}
2.73	105	8.34	1.36	6.57	4.09	0.788	7.34	1.07	0.38
	205	8.51	1.16	7.28	0.78	0.855	8.62	1.05	0.04
	305	7.60	1.05	6.44	1.08	0.848	9.54	1.17	0.23
3.64	107.5	4.66	1.52	2.94	2.02	0.631	6.58	1.92	0.39
	207.5	5.53	1.11	4.22	2.01	0.763	9.04	1.62	0.12
	307.5	4.77	1.00	3.59	1.72	0.754	9.96	1.87	0.25
4.55	110	2.32	1.33	0.06	9.22	0.279	7.49	3.85	0.56
	210	2.80	1.10	0.86	8.42	0.306	9.11	3.19	0.33
	310	3.11	0.97	1.88	2.64	0.604	10.35	2.87	0.20

The cleaning regime consisted of rinsing the membrane system with: distilled water (10 minutes), ~1.7% NaOH solution (10 minutes), distilled water (5 minutes), 2% HNO_3 solution (5 minutes), distilled water (5 minutes), 2% HNO_3 solution (10 minutes), distilled water (10 minutes). After cleaning, water permeation measurements have been performed again. This procedure allowed to assess transport resistances through the membrane.

3. RESULTS AND DISCUSSION

The test results have been obtained in the form of permeation curves, i.e. permeate flux versus filtration time. Based on the experimental data, the transport resistances through the membrane have been determined using the resistance-in-series model and the results have been presented in Table 3. Moreover, the values of hydraulic permeability for clean membrane and fouled membrane have been presented. Afterwards, the pore blocking models were applied to identify membrane fouling mechanism during chicken egg white ultrafiltration.

3.1. Resistance-in-series model

This model is based on Darcy's law, which is an expression of relations between transmembrane pressure, permeate flux and the total hydraulic resistance (Bader and Veenstra, 1996). Darcy's law has been presented as Eq. (1).

$$J_P = \frac{TMP}{\mu \cdot R_T} = \frac{TMP}{\mu \cdot (R_M + R_F + R_{RES})} \tag{1}$$

The total hydraulic resistance R_T is a sum of individual mass transport resistances that take place in membrane filtration, e.g. clean membrane resistance, R_M, fouling resistance, R_F and residual resistance, R_{RES}. The results obtained from the experimental data, calculated according to Eq. (1) are shown in Table 3. Additionally, the ratio of the fouling resistance to the total resistance has been calculated. Fouling resistance versus transmembrane pressure and cross-flow velocity is presented in Fig. 2.

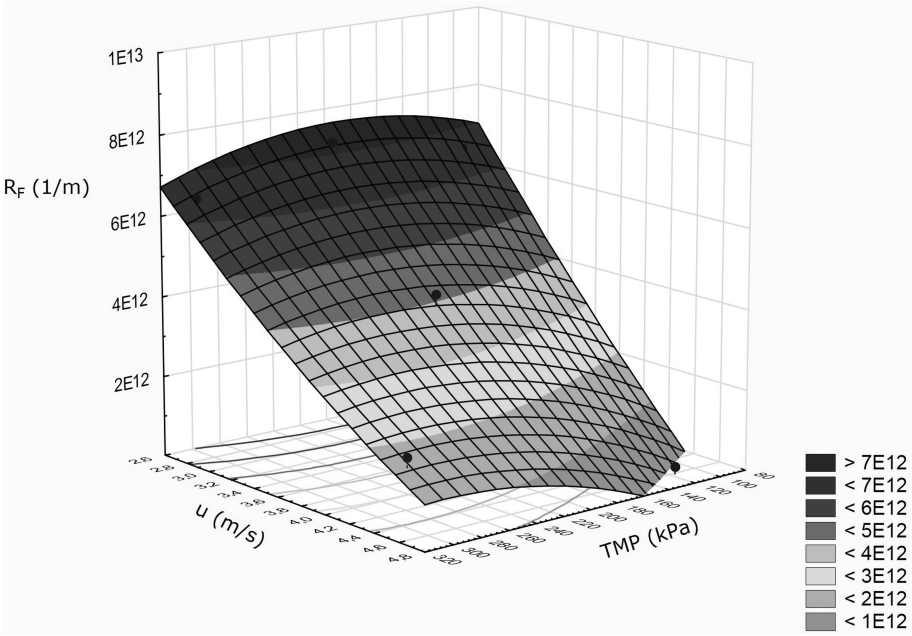

Fig. 2. Fouling resistance R_F versus cross-flow velocity u and transmembrane pressure TMP with 3D surface approximation

The highest fouling resistance has been observed at $u = 2.73$ m/s and $TMP = 205$ kPa, and the lowest at $u = 4.55$ m/s and $TMP = 110$ kPa. The ratio of the fouling resistance to the total resistance grew with a decrease of cross-flow velocity. Hydraulic permeability values have been calculated according to Eq. (2) and presented in Table 3.

$$L = \frac{J_P}{TMP} \tag{2}$$

Hydraulic permeability L $(\mathrm{m}^3/(\mathrm{m}^2 \cdot \mathrm{s} \cdot \mathrm{Pa}))$ with subscript M stands for clean membrane permeability, while subscript P stands for fouled membrane permeability. The value achieved for fouled membrane is much lower than that for clean membrane in all of the runs.

3.2. Retention coefficient

For each of the test runs, retention coefficient has been calculated using Eq. (3).

$$R_{coef} = 1 - \frac{C_P}{C_F} \tag{3}$$

The values of retention coefficient have been presented in Table 3. The values achieved are relatively low (only one test run result was above 0.5), which may be caused by the difference between the molecular weight of the main component of chicken egg white (45 kDa) and the cut-off value of the membrane (150 kDa). The research shows that with increasing feed rate, the fouling resistance decreases and higher values of permeate flow are possible to obtain. At the same time, the protein retention coefficient increases, which means that less protein passes through the separation layer and the retentate is getting concentrated. The increase of pressure does not have a clear effect on the fouling resistance and the retention coefficient in the system. This issue will be the subject of further studies.

The main goal of the study was to provide information about mass transfer mechanisms and transport resistances in membrane separation process of chicken egg white solutions. The influence of operating parameters (*u, TMP*) on the fouling resistance value has been presented in Fig. 2. The parameter that holds the greatest influence on fouling resistance is the cross-flow velocity *u*.

3.3. Pore blocking models

Four models of membrane pore blocking during dead-end filtration were developed by Hermia (Hermia, 1985) and later adapted to cross-flow filtration by Field et al. (Field et al., 1995). The type of the adequate pore blocking model depends on the value of n parameter in a general Eq. (4) (Hermia, 1985; Kumar et al., 2016).

$$\frac{d^2t}{dV^2} = K\left(\frac{dt}{dV}\right)^n \tag{4}$$

For cross-flow filtration, Eq. (4) was modified into Eq. (5) (Vincent Vela et al., 2009; Field et al., 1995; Corbatón-Báguena et al., 2015).

$$-\frac{dJ_P}{dt} = K(J_P - J_{Pss})J_P^{2-n} \tag{5}$$

Visual representations of the four models are shown in Fig. 3.

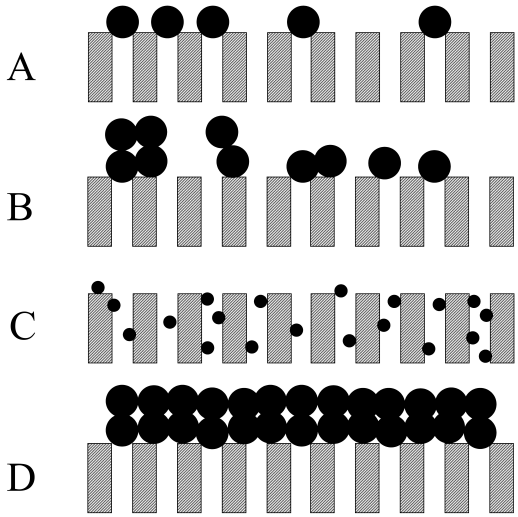

Fig. 3. Pore blocking models: A – complete pore blocking, B – intermediate pore blocking, C – standard pore blocking, D – cake filtration

Pore blocking models have been applied to experimental data using STATISTICA software. For a complete and intermediate pore blocking models, cross-flow adaptations have been used. For a standard pore blocking model and the cake filtration model, classic dead-end filtration models have been used. To acquire the value of pore blocking model parameters K with respective indexes, nonlinear regression model has been used along with the Gauss-Newton estimation method, where regression coefficient R (–) was calculated. Additionally, average relative error δ (%) (Eq. (6)) was estimated, and both parameters have been used for rating the quality fit of the pore blocking model.

$$\delta = \frac{1}{N}\sum_{i=1}^{N}\left|\frac{J_{Pexp,i} - J_{Pcalc,i}}{J_{Pexp,i}}\right| \cdot 100 \tag{6}$$

Complete blocking (n = 2)

This model assumes that every particle that goes into the membrane module and reaches membrane surface blocks single pore entrances completely. One molecule can block only one pore, and another molecule will not settle on the previous one. Permeate flows only through unaffected pores. This type of blocking happens when the size of membrane pores is smaller than the size of molecules in the solution (Vincent Vela et al., 2009). The equation for the permeate flux as a function of time is as follows:

$$J_P = J_0 \cdot e^{-K_b t} \tag{7}$$

This model was adapted for cross-flow filtration by adding a representation of molecule removal rate from the pore entrances:

$$J_P = J_{Pss} + (J_0 - J_{Pss})e^{-K_b J_0 t} \tag{8}$$

Model parameters and results obtained for complete pore blocking model are presented in Table 4.

Table 4. Results obtained for complete pore blocking model

u [m/s]	TMP [kPa]	$J_0 \cdot 10^5$ [m^3/(m^{2}s)]	$J_{Pss} \cdot 10^5$ [m^3/(m^{2}s)]	K_b [m^{-1}]	δ [%]	R
2.73	105	1.41	1.12	18.88	6.46	0.741
	205	4.74	2.15	50.71	4.07	0.937
	305	4.93	3.58	6.19	2.65	0.954
3.64	107.5	2.68	2.06	17.25	4.85	0.865
	207.5	5.70	3.35	8.22	2.83	0.976
	307.5	8.62	5.76	7.10	1.58	0.983
4.55	110	7.18	4.23	4.47	4.87	0.923
	210	8.61	6.71	5.68	3.13	0.930
	310	13.49	8.91	3.50	2.29	0.977

Experimental data for cross-flow velocity 4.55 m/s and different transmembrane pressure values, along with appropriate complete pore blocking fit are visible in Fig. 4.

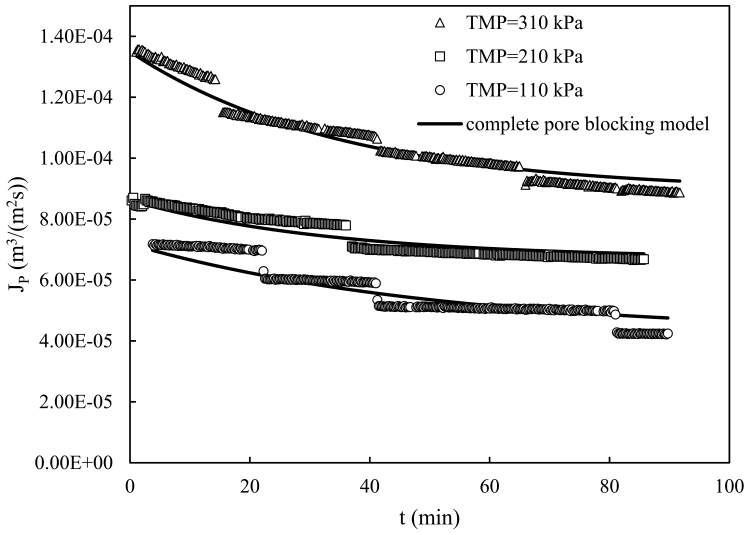

Fig. 4. Experimental data of $J_P = f(t)$ with fitted complete pore blocking model ($u = 4.55$ m/s, $TMP = 110$ kPa; 210 kPa; 310 kPa)

For complete pore blocking model, the value of R coefficient exceeds 0.900 in most of the runs. The average relative error is below 5% in eight out of nine runs. These values indicate that the model gives a good fit to experimental data, which is also shown in Fig. 4.

Intermediate blocking (n = 1)

This model assumes that pores are blocked by molecules, but in contrast to the complete pore blocking model, other molecules can be deposited on the top of the molecules originally blocking the pore entrances.

Also, molecules do not necessarily have to block pores landing on membrane surface (Vincent Vela et al., 2009). For dead-end filtration, intermediate blocking model is defined by Eq. (9).

$$J_P = \frac{1}{\frac{1}{J_0} + K_i t} \tag{9}$$

Cross-flow adaptation of this model is as follows (Vincent Vela et al., 2009):

$$J_P = \frac{J_0 J_{Pss} e^{K_i J_{Pss} t}}{J_{Pss} + J_0 \left(e^{K_i J_{Pss} t} - 1\right)} \tag{10}$$

The results of intermediate pore blocking model approximation are presented in Table 5 and Fig. 5.

Table 5. Results obtained for intermediate pore blocking model

u [m/s]	TMP [kPa]	$J_0 \cdot 10^5$ [m^3/(m^{2}s)]	$J_{Pss} \cdot 10^5$ [m^3/(m^{2}s)]	K_b [m^{-1}]	δ [%]	R
2.73	105	1.41	1.12	20.05	6.59	0.731
	205	4.74	2.15	67.59	3.12	0.951
	305	4.93	3.58	6.90	2.92	0.944
3.64	107.5	2.68	2.06	18.98	5.10	0.853
	207.5	5.70	3.35	9.98	3.53	0.964
	307.5	8.62	5.76	8.38	1.70	0.984
4.55	110	7.18	4.23	5.22	5.30	0.906
	210	8.61	6.71	6.25	3.35	0.920
	310	13.49	8.91	4.10	2.59	0.968

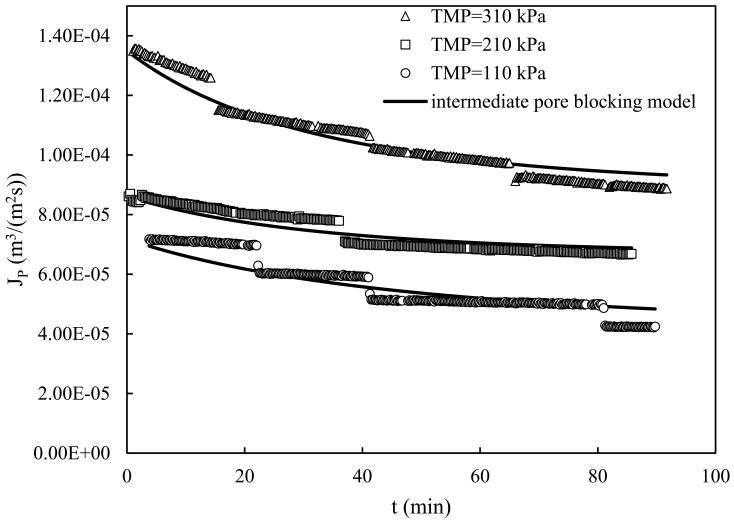

Fig. 5. Experimental data of $J_P = f(t)$ with fitted intermediate pore blocking model ($u = 4.55$ m/s, $TMP = 110$ kPa; 210 kPa; 310 kPa)

Analysis of the results obtained shows that intermediate pore blocking model gives also a good fit to the experimental data. Average relative error is over 5% in the runs where the transmembrane pressure has been in the range of 105–110 kPa. Correlation coefficient is below 0.900 only for two runs ($u = 2.73$ m/s, $TMP = 105$ kPa; $u = 3.64$ m/s, $TMP = 107.5$ kPa). Comparing these results with the ones acquired with the

use of complete pore blocking model, slightly better approximation was achieved. Correlation coefficient is higher for complete pore blocking model in 7 out of 9 runs, and the standard error is lower in all of the runs but one ($u = 2.73$ m/s, $TMP = 205$ kPa).

Standard blocking (n = 3/2)

Standard pore blocking model assumes that particles settle on pore walls, which causes a decrease in pore volume. Molecules can be either simply deposited on the walls, or adsorbed on their surface. Membrane pore volume is reduced proportionally to the amount of permeate volume (Vincent Vela et al., 2009). The equation for standard blocking model in cross flow filtration is the same as that in dead end filtration and is presented below (Vincent Vela et al., 2009).

$$J_P = \frac{J_0}{\left(J_0 + J_0^{1/2} K_s t\right)^2} \tag{11}$$

The results achieved by applying the standard pore blocking model to experimental data are listed in Table 6 and Fig. 6.

Table 6. Results obtained for standard pore blocking model

u [m/s]	TMP [kPa]	$J_0 \cdot 10^5$ [m^3/(m^{2}s)]	$J_{Pss} \cdot 10^5$ [m^3/(m^{2}s)]	K_b [m^{-1}]	δ [%]	R
2.73	105	1.41	1.12	1.37	96.11	0.000
	205	4.74	2.15	0.98	93.53	0.000
	305	4.93	3.58	0.74	96.50	0.000
3.64	107.5	2.68	2.06	4.39	99.67	0.000
	207.5	5.70	3.35	0.55	94.44	0.000
	307.5	8.62	5.76	2.55	99.02	0.000
4.55	110	7.18	4.23	0.32	91.92	0.000
	210	8.61	6.71	5.38	99.54	0.000
	310	13.49	8.91	0.94	98.00	0.000

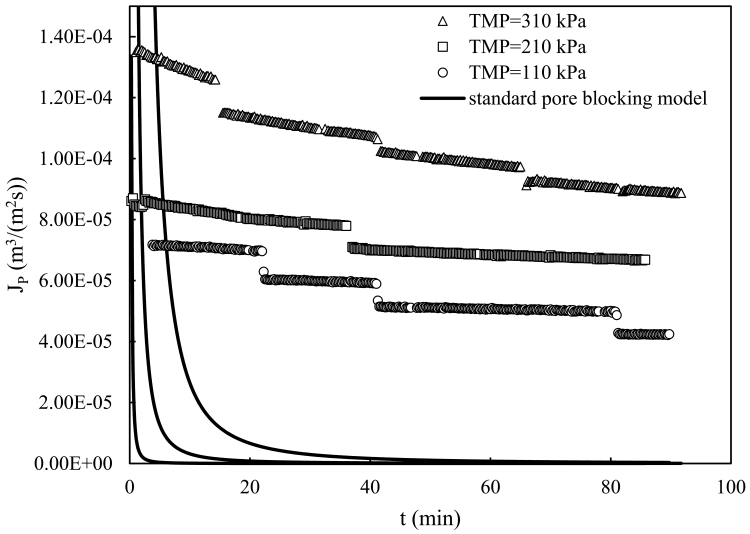

Fig. 6. Experimental data of $J_P = f(t)$ with fitted standard pore blocking model ($u = 4.55$ m/s, $TMP = 110$ kPa; 210 kPa; 310 kPa)

In case of standard pore blocking model, the correlation coefficient is equal to zero in each run and the average relative error is over 90% for all runs. A graphic representation of this model also confirms that this model is not suitable for the experimental data achieved during ultrafiltration of chicken egg white.

Cake filtration (n = 0)

Molecules of the solute bigger than pore entrance size aggregate and create a layer that blocks the flow completely. The cake layer gets thicker over time (Vincent Vela et al., 2009). In dead-end filtration, cake filtration model is represented by Eq. (12) (Vincent Vela et al., 2009).

$$J_P = \frac{J_0}{\left(1 + 2K_c J_0^2 t\right)^{1/2}} \tag{12}$$

In the ultrafiltration process, cake filtration does not occur in the same way as in microfiltration. The particles are smaller and they do not enter the membrane pores, but form a gel layer over the membrane surface instead. For UF this model is called the gel layer formation and for cross-flow technique Eq. (13) was developed (Field et al., 1995; Vincent Vela et al., 2009).

$$t = \frac{1}{K_g J_{Pss}^2} \ln\left[\left(\frac{J_P}{J_0}\frac{J_0 - J_{Pss}}{J_P - J_{Pss}}\right) - J_{Pss}\left(\frac{1}{J_P} - \frac{1}{J_0}\right)\right] \tag{13}$$

The gel layer formation model presented in Eq. (13) provided no fitting at all, and for that reason the classic cake filtration model for dead-end process has been used. The results achieved with this model are presented in Table 7.

Table 7. Results obtained for cake filtration model

u [m/s]	TMP [kPa]	$J_0 \cdot 10^5$ [m^3/(m^{2}s)]	$J_{Pss} \cdot 10^5$ [m^3/(m^{2}s)]	K_b [m^{-1}]	δ [%]	R
2.73	105	1.41	1.12	234850	5.55	0.788
	205	4.74	2.15	412417	12.10	0.581
	305	4.93	3.58	27949	1.48	0.984
3.64	107.5	2.68	2.06	108905	3.80	0.905
	207.5	5.70	3.35	55888	1.96	0.987
	307.5	8.62	5.76	19536	3.20	0.934
4.55	110	7.18	4.23	25641	4.70	0.931
	210	8.61	6.71	10124	2.17	0.960
	310	13.49	8.91	7180	1.62	0.987

In the case of cake filtration model, the value of the correlation coefficient is below 0.900 for only two runs. The average relative error exceeds 5% also in two runs. A comparison of the results obtained for the complete pore blocking model and for the cake filtration model has revealed that the cake filtration model has given a better fit than the complete pore blocking model in most of the experimental runs. A graphical representation of the obtained model fits has been presented in Fig. 7.

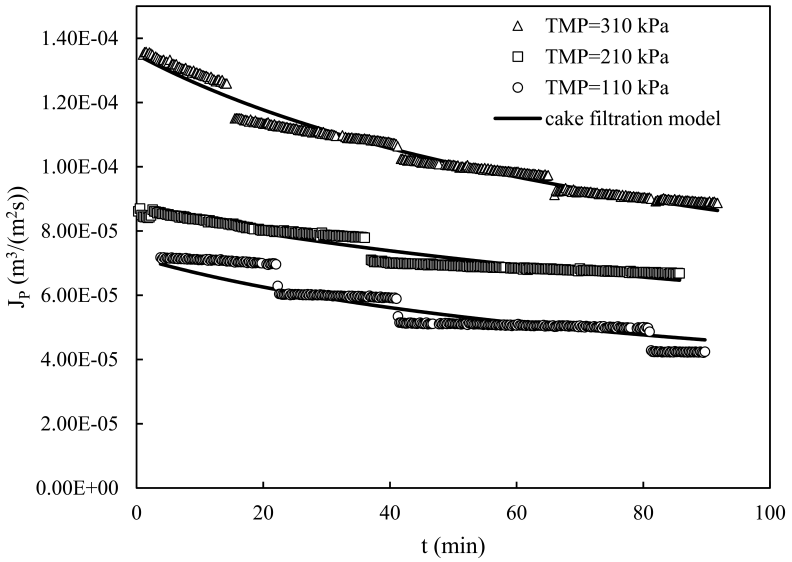

Fig. 7. Experimental data of $J_P = f(t)$ with fitted cake filtration model ($u =$ 4.55 m/s, $TMP =$ 110 kPa; 210 kPa; 310 kPa)

4. CONCLUSIONS

During ultrafiltration of chicken egg white solution, a permeate flux decline with time has been observed. The reason for this phenomenon is membrane fouling – in general, caused by particles of the solute remaining on the membrane surface. Fouling results in an additional transport resistance in the filtration process. Total resistance and its components (fouling resistance, clean membrane resistance and residual resistance) were calculated using a resistance-in-series model. The highest values of the fouling resistance have been observed at the lowest value of the cross-flow velocity ($u = 2.73$ m/s). Maximum fouling resistance has been noted at a middle value of the transmembrane pressure ($u = 2.73$ m/s, $TMP = 205$ kPa).The lowest values of fouling resistance have been achieved at the highest value of the cross-flow velocity ($u = 4.55$ m/s). Minimum fouling resistance has been noted at the lowest value of the transmembrane pressure ($u = 4.55$ m/s, $TMP = 110$ kPa).

The retention coefficient values achieved are relatively low (0.04–0.56). The protein retention coefficient increases with the cross-flow velocity in the membrane module, and the transmembrane pressure does not have a clear impact on this value.

Particles can reside on the membrane surface in many different ways. Four pore blocking models (complete pore blocking model, intermediate pore blocking model, standard pore blocking model and cake filtration model) have been fitted to the experimental data and an identification of the fouling mechanism was attempted. The analysis of the achieved results indicates that for the most of the runs, the cake filtration model provided the best fit to the experimental data, so this mechanism of pore blocking may be considered as a dominant one. Complete and intermediate pore blocking models have also given a good fit to the experimental data, so it may imply that these pore blocking mechanisms also occur in the process but not as intensively as the cake filtration mechanism. The standard pore blocking has not given satisfying results, so it either is nonexistent or occurs to a very limited extend. The results obtained in the study indicate that the pore blocking mechanism in the process of chicken egg white protein ultrafiltration is a complex one.

SYMBOLS

C_F concentration of solute in feed stream, g/L
C_P oncentration of solute in permeate stream, g/L
J_0 initial permeate flux, $m^3/(m^2s)$
J_P permeate flux, $m^3/(m^2s)$
J_{Pss} steady-state permeate flux, $m^3/(m^2s)$
K pore blocking model constant, m^{-1} (for complete pore blocking, intermediate pore blocking and cake filtration models), or $m^{-1/2}s^{-1/2}$ (for standard pore blocking model)
L_M hydraulic permeability of clean membrane, $m^3/(m^2sPa)$
L_P hydraulic permeability of fouled membrane, $m^3/(m^2sPa)$
n specific parameter of pore blocking, –
R_{coef} retention coefficient, –
R_F fouling resistance, m^{-1}
R_M clean membrane resistance, m^{-1}
R_{RES} residual resistance, m^{-1}
R_T total hydraulic resistance, m^{-1}
t time of permeation, s
TMP transmembrane pressure, Pa
u cross-flow velocity, m/s
V collected permeate volume, m^3

Greek letters

δ average relative error, %
μ dynamic viscosity of the solution, Pas

Subscripts

calc calculated
exp experimental
b complete
c cake
i intermediate
s standard

REFERENCES

Agana B.A., Reeve D., Orbell J.D., 2013. Performance optimization of a 5 nm TiO_2 ceramic membrane with respect to beverage production wastewater. *Desalination*, 311, 162–172. DOI: 10.1016/j.desal.2012.11.027.

Almandoz C., Pagliero C., Ochoa A., Marchese J., 2010. Corn syrup clarification by microfiltration with ceramic membranes. *J. Membr. Sci.*, 363, 87–95. DOI: 10.1016/j.memsci.2010.07.017.

Bader M.S.H., Veenstra J.N., 1996. Analysis of concentration polarization phenomenon in ultrafiltration under turbulent flow conditions. *J. Membr. Sci.*, 114, 139–148. DOI: 10.1016/0376-7388(95)00136-0.

Balyan U., Sarkar B., 2018. Analysis of flux decline using sequential fouling mechanisms during concentration of *Syzygium cumini* (L.) leaf extract. *Chem. Eng. Res. Des.*, 130, 167–183. DOI: 10.1016/j.cherd.2017.12.015.

Bodzek M., Bohdziewicz J., Konieczny K., 1997. *Techniki membranowe w ochronie środowiska*. Wydawnictwo Politechniki Śląskiej.

Corbatón-Báguena M. J., Álvarez-Blanco S., Vincent-Vela M.C., 2015. Fouling mechanisms of ultrafiltration membranes fouled with whey model solutions. *Desalination*, 360, 87–96. DOI: 10.1016/j.desal.2015.01.019.

Corbatón-Báguena M.J., Álvarez-Blanco S., Vincent-Vela M.C., 2018. Evaluation of fouling resistances during the ultrafiltration of whey model solutions. *J. Cleaner Prod.*, 172, 358–367. DOI: 10.1016/j.jclepro.2017.10.149.

de Barros S.T.D., Andrade C.M.G., Mendes E.S., Peres L., 2003. Study of fouling mechanism in pineapple juice clarification by ultrafiltration. *J. Membr. Sci.*, 215, 213–224. DOI: 10.1016/S0376-7388(02)00615-4.

Ehsani N., Parkkinen S., Nyström M., 1997. Fractionation of natural and model egg-white protein solutions with modified and unmodified polysulfone UF membranes. *J. Membr. Sci.*, 123, 105-119. DOI: 10.1016/S0376-7388(96)00207-4.

Fane A.G., Wang R., Jia Y., 2011. Membrane technology: Past, present and future. In: Wang L.K., Chen J.P., Hung YT., Shammas N.K. (Eds.) *Membrane and Desalination Technologies. Handbook of Environmental Engineering*, Vol 13. Humana Press, Totowa, NJ, 1–45. DOI: 10.1007/978-1-59745-278-6_1.

Field R.W., Wu D., Howell J.A., Gupta B.B., 1995. Critical flux concept for microfiltration fouling. *J. Membr. Sci.*, 100, 259–272. DOI: 10.1016/0376-7388(94)00265-Z.

Gabruś E., 2016. *Wybrane metody adsorpcyjno-membranowe w inżynierii procesowej*. BEL Studio.

Ghosh R., Cui Z.F., 1998. Fractionation of BSA and lysozyme using ultrafiltration: effect of pH and membrane pretreatment. *J. Membr. Sci.*, 139, 17–28. DOI: 10.1016/S0376-7388(97)00236-6.

Hermia J., 1985. Blocking filtration. Application to non-Newtonian fluids. In: Rushton A. (Ed.), *Mathematical models and design methods in solid-liquid separation*. Springer Netherlands, 83–89. DOI: 10.1007/978-94-009-5091-7_5.

Huisman I.H., Prádanos P., Hernández A., 2000. The effect of protein–protein and protein–membrane interactions on membrane fouling in ultrafiltration. *J. Membr. Sci.*, 179, 79–90. DOI: 10.1016/S0376-7388(00)00501-9.

Jana S., Purkait M.K., Mohanty K., 2011. Clay supported polyvinyl acetate coated composite membrane by modified dip coating method: Application for the purification of lysozyme from chicken egg white. *J. Membr. Sci.*, 382, 243–251. DOI: 10.1016/j.memsci.2011.08.011.

Kumar R.V., Goswami L., Pakshirajan K., Pugazhenthi G., 2016. Dairy wastewater treatment using a novel low cost tubular ceramic membrane and membrane fouling mechanism using pore blocking models. *J. Water Process Eng.*, 13, 168–175. DOI: 10.1016/j.jwpe.2016.08.012.

Li M., Zhao Y., Zhou S., Xing W., 2010. Clarification of raw rice wine by ceramic microfiltration membranes and membrane fouling analysis. *Desalination*, 256, 166–173. DOI: 10.1016/j.desal.2010.01.018.

Lu J., Wan Y., Cui Z., 2005. Fractionation of lysozyme and chicken egg albumin using ultrafiltration with 30-kDa commercial membranes. *Ind. Eng. Chem. Res.*, 44, 7610–7616. DOI: 10.1021/ie049042c.

Lu J., Wan Y., Cui Z., 2006. Strategy to separate lysozyme and ovalbumin from CEW using UF. *Desalination*, 200, 477–479. DOI: 10.1016/j.desal.2006.03.402.

Matsumoto Y., Ito N., Inui T., 1996. Characteristics of ovalbumin gel layer formed on ceramic microfiltration membranes. *J. Chem. Eng. Jpn.*, 29, 933–938. DOI: 10.1252/jcej.29.933.

Muca R., Piątkowski W., Antos D., 2017. A shortcut method for evaluation of protein deposition onto the membrane surface in crossflow ultrafiltration. *Eng. Life Sci.*, 17, 370–381. DOI: 10.1002/elsc.201500159.

Pabby A.K., Rizvi S.S.H., Requena A.M.S., 2008. *Handbook of membrane separations: Chemical, pharmaceutical, food, and biotechnological applications*. Taylor & Francis.

Prádanos P., Hernández A., Calvo J.I., Tejerina F., 1996. Mechanisms of protein fouling in cross-flow UF through an asymmetric inorganic membrane. *J. Membr. Sci.*, 114, 115–126. DOI: 10.1016/0376-7388(95)00324-X.

Rayess Y.E., Albasi C., Bacchin P., Taillandier P., Mietton-Peuchot M., Devatine A., 2011. Cross-flow microfiltration of wine: Effect of colloids on critical fouling conditions. *J. Membr. Sci.*, 385–386, 177–186. DOI: 10.1016/j.memsci.2011.09.037.

Samaei S. M., Gato-Trinidad S., Altaee A., 2018. The application of pressure-driven ceramic membrane technology for the treatment of industrial wastewaters – A review. *Sep. Purif. Technol.*, 200, 198–220. DOI: 10.1016/j.seppur.2018.02.041.

Tung K.-L., Hu C.-C., Li C.-L., Chuang C.-J., 2007. Investigating protein crossflow ultrafiltration mechanisms using interfacial phenomena. *J. Chin. Inst. Chem. Eng,*, 38, 303–311. DOI: 10.1016/j.jcice.2007.01.005.

Vincent Vela M.C., Álvarez Blanco S., Lora García J., Bergantiños Rodríguez E., 2009. Analysis of membrane pore blocking models adapted to crossflow ultrafiltration in the ultrafiltration of PEG. *Chem. Eng. J.,* 149, 232–241. DOI: 10.1016/j.cej.2008.10.027.

Wan Y., Lu J., Cui Z., 2006. Separation of lysozyme from chicken egg white using ultrafiltration. *Sep. Purif. Technol.*, 48, 133–142. DOI: 10.1016/j.seppur.2005.07.003.

Yin N., Zhong Z., Xing W., 2013. Ceramic membrane fouling and cleaning in ultrafiltration of desulfurization wastewater. *Desalination*, 319, 92–98. DOI: 10.1016/j.desal.2013.03.028.

Youravong W., Li Z., Laorko A., 2010. Influence of gas sparging on clarification of pineapple wine by microfiltration. *J. Food Eng.*, 96, 427–432. DOI: 10.1016/j.jfoodeng.2009.08.021.

Received 28 April 2018
Received in revised form 23 July 2018
Accepted 24 July 2018